The Astrophysical Journal Letters, 789:L43 (4pp), 2014 July 10 doi:10.1088/2041-8205/789/2/L43

WHY ARE THE MAGNETIC FIELD DIRECTIONS MEASURED BY *VOYAGER 1* ON BOTH SIDES OF THE HELIOPAUSE SO SIMILAR?

J. Grygorczuk, A. Czechowski, and S. Grzedzielski
Space Research Centre, Warsaw, Poland; jolagry@cbk.waw.pl

Received 2014 April 3; accepted 2014 June 16; published 2014 June 27

ABSTRACT

The solar wind carves a cavity in the interstellar plasma bounded by a surface, called the heliopause (HP), that separates the plasma and magnetic field of solar origin from those of interstellar origin. It is now generally accepted that in 2012 August *Voyager 1* (*V1*) crossed that boundary. Unexpectedly, the magnetic fields on both sides of the HP, although theoretically independent of each other, were found to be similar in direction. This delayed the identification of the boundary as the HP and led to many alternative explanations. Here, we show that the *Voyager 1* observations can be readily explained and, after the *Interstellar Boundary Explorer* (*IBEX*) discovery of the ribbon, could even have been predicted. Our explanation relies on the fact that the *Voyager 1* and undisturbed interstellar field directions (which we assume to be given by the *IBEX* ribbon center (RC)) share the same heliolatitude ($\sim 34\overset{\circ}{.}5$) and are not far separated in longitude (difference $\sim 27^\circ$). Our result confirms that *Voyager 1* has indeed crossed the HP and offers the first independent confirmation that the *IBEX* RC is in fact the direction of the undisturbed interstellar magnetic field. For *Voyager 2*, we predict that the difference between the inner and outer magnetic field directions at the HP will be significantly larger than that observed by *Voyager 1* ($\sim 30^\circ$ instead of $\sim 20^\circ$), and that the outer field direction will be close to the RC.

Key words: ISM: magnetic fields – Sun: heliosphere

1. INTRODUCTION

In 2012 August, *Voyager 1* (*V1*) crossed the heliopause (HP) and entered the local interstellar medium (LISM; Burlaga et al. 2013; Stone et al. 2013). Contrary to expectations, the change in the magnetic field direction across the HP was small (Burlaga et al. 2013) ($\sim 20^\circ$). As a result, the identification of the boundary as the HP remained in doubt. This led to speculations concerning the existence of an unexpected transition layer at the HP that allows an enhanced exchange of energetic particles with the interstellar medium while conserving magnetic field characteristics typical of the heliosheath (Fisk & Gloeckler 2013; Florinski 2013; McComas & Schwadron 2012; Stone et al. 2013; Schwadron & McComas 2013). Only the detection of electron plasma oscillations, which allowed us to evaluate the local plasma density at *V1* in 2013, with values characteristic of the LISM, provided strong evidence that the spacecraft has already crossed the HP (Gurnett et al. 2013). However, it is still not understood why the magnetic field direction observed beyond the HP is so close to the field measured in the inner heliosheath, and attempts are still being made to answer this question (Schwadron & McComas 2013; Fisk & Gloeckler 2013; Florinski 2013; Opher & Drake 2013; Borovikov & Pogorelov 2014).

In this Letter, we show how this observation can be explained in a simple and natural way if the undisturbed interstellar magnetic field (ISMF) far from the heliosphere points to the *Interstellar Boundary Explorer* (*IBEX*) ribbon center (RC; Funsten et al. 2009). The ribbon is an almost circular arc of enhanced energetic neutral atoms emission in the sky discovered by the *IBEX* (McComas et al. 2009; Funsten et al. 2009). The RC is widely interpreted as the direction of the undisturbed ISMF (Funsten et al. 2009; McComas et al. 2013; Funsten et al. 2013). We use the RC location from Funsten et al. (2009) and McComas et al. (2009) (see Table 1). The recent energy-averaged RC position (Funsten et al. 2013) differs from this location only by $1\overset{\circ}{.}6$. A change by this amount would not significantly affect our results.

There are two crucial aspects of our explanation. First, the heliolatitudes of *V1* and the undisturbed ISMF happen to be approximately the same ($\sim 34\overset{\circ}{.}5$; see Table 1), with a small angular distance between the two directions ($\sim 27^\circ$). Second, for a strong interstellar field, the draping around the HP has a simple structure, the evolution of which (in the region of HP not far from the undisturbed field direction) can be traced for the field magnitude decreasing toward realistic values.

The essence of our argument is presented in Figure 1. The *V1* and ISMF (RC) directions are shown on a sky map in orthogonal projection and Sun-centered equatorial (heliographic inertial) coordinates.[1] From *V1* observations, we know (Burlaga et al. 2013) that the magnetic field on the inner side of the HP is very close to the Parker spiral, that is, to the $-T$ direction in the Radial-Tangential-Normal (RTN) system.[2] Projected on the sky map, the solar magnetic field line is tangent to the heliographic parallel passing through the *V1* position. $B_{\rm IN}$ and $B_{\rm OUT}$ denote the directions of the magnetic field measured by *V1* before and after crossing the HP, respectively.

The projection of the ISMF line passing through the *V1* position must link this point with the direction of the unperturbed ISMF (RC). If the draping pattern is such that the projected ISMF line reaches RC from *V1* with little change in direction, then the ISMF at *V1* must be approximately parallel to the inner field simply because *V1* and RC have the same heliolatitude.

2. SIMPLE DRAPING MODEL

The simplest ("idealized") draping model with this property is illustrated in Figure 1, where the selected draped ISMF field lines are shown as thick blue lines. We chose one of them to pass through the *V1* position and another through the *Voyager 2* (*V2*) position. In this model, based on the well-known solution

[1] http://omniweb.gsfc.nasa.gov/coho/helios/coor_des.html

[2] http://www.srl.caltech.edu/ACE/ASC/coordinate_systems.html. The transformation from heliographic inertial to RTN coordinates follows from Franz & Harper (2002).

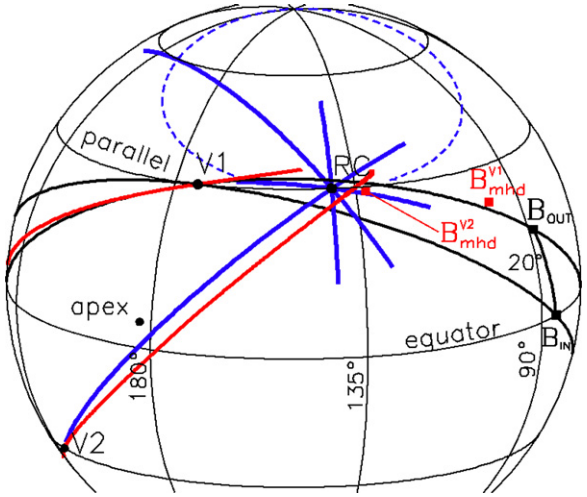

Figure 1. Sky map in orthogonal projection and heliographic inertial coordinates. We show *Voyager 1* (*V1*), *Voyager 2* (*V2*), *IBEX* ribbon center (RC), interstellar inflow direction (apex), and magnetic field directions measured by *V1* before and after crossing the heliopause (B_{IN} and B_{OUT}, respectively). Two great circles (black) link *V1* with B_{OUT} and B_{IN} (the latter is tangent to the heliographic parallel at *V1*). Thick blue lines are the interstellar magnetic field lines in the idealized draping model. The dashed blue oval is a locus of points where the idealized draped interstellar field lines become tangent to the local heliographic parallel (illustrated by the extended field line in the north). The thick red lines are the draped magnetic field lines obtained from our simulation for the 4 μG case. The red squares (B^{V1}_{mhd} and B^{V2}_{mhd}) are the directions of the interstellar field just outside the heliopause in the directions of *V1* and *V2* for the same simulation.

Table 1
Characteristic Directions in Galactic (GAL), Solar Ecliptic (SE), Solar Equatorial (HGI[a]), and RTN[b] Coordinates (J2000)

	GAL		SE		HGI[a]		RTN[b]	
	Lon (deg)	Lat (deg)	Lon (deg)	Lat (deg)	Lon (deg)	Lat (deg)	Lon (deg)	Lat (deg)
V1	32.7	28.1	254.9	35.0	174.1	34.5		
V2	342.1	−31.2	289.4	−34.2	217.2	−30.0		
RC(= B_{IS})	32.9	55.3	221.0	39.0	140.9	34.6		
apex	5.3	12.0	259.0	4.98	182.6	5.4		
B_{IN}	232.0	60.4	159.6	7.2	83.9	0.0	270.	0.
B_{OUT}	197.2	75.1	163.7	26.0	88.0	18.8	284.	13.
B^{V1}_{MHD} 2.7μG[c]	155.	80.	169.	35.	93.	28.	293.	18.
B^{V1}_{MHD} 3μG[c]	164.	73.	161.	35.	95.	28.	295.	17.
B^{V1}_{MHD} 4μG[c]	168.	53.	137.	34.	100.	27.	298.	13.
B^{V1}_{MHD} 20.0μG	28.	63.	211.	36.	132.	31.	325.	3.
B^{V1}_{MHD} 3μG[d]	159.	71.	159.	37.	93.	30.	294.	19.
B^{V1}_{MHD} 4μG[d]	126.	83.	176.	36.	99.	29.	299.	16.
B^{V2}_{MHD} 2.7μG[c]	36.	65.	208.	39.	129.	34.	253.	29.
B^{V2}_{MHD} 3μG[c]	35.	64.	209.	39.	130.	33.	254.	30.
B^{V2}_{MHD} 4μG[c]	34.	62.	212.	39.	132.	34.	256.	31.
B^{V2}_{MHD} 20.0μG	30.	53.	224.	37.	143.	33.	265.	36.
B^{V2}_{MHD} 3μG[d]	37.	62.	212.	40.	133.	35.	255.	32.
B^{V2}_{MHD} 4μG[d]	35.	60.	215.	40.	135.	35.	257.	33.

Notes.
[a] http://omniweb.gsfc.nasa.gov/coho/helios/coor_des.html
[b] http://www.srl.caltech.edu/ACE/ASC/coordinate_systems.html
[c] Table 2 solar wind case 400/750.
[d] Table 2 solar wind case 500/750.

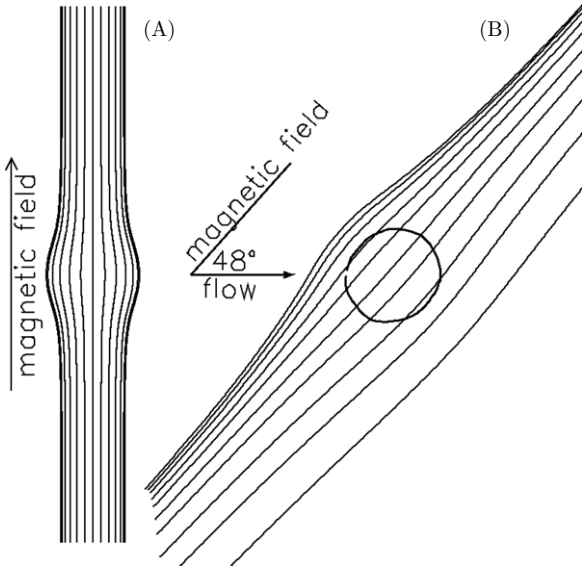

Figure 2. Draped interstellar magnetic field lines: (a) in Parker's solution (star at rest relative to the interstellar medium with insignificant plasma density), and (b) obtained from 3D MHD simulations for spherically symmetric solar wind and interstellar magnetic field of 20 μG, inclined 48° to interstellar plasma flow (projection on a plane containing interstellar flow and field vectors).

by Parker (Parker 1961; see also Figure 2), the projected lines are arcs of great circles and originate in the undisturbed ISMF direction (RC).

In Parker's solution, the star is at rest relative to the interstellar medium with insignificant plasma density and strong magnetic field. The stellar wind plasma flows away from the star, forming two streams, parallel and anti-parallel to the ISMF direction. Below, we will show, based on our 3DMHD simulations (Czechowski et al. 2014), that the same idealized draping model can be regarded as the high ISMF strength limit for the case of the Sun, which is moving through the medium including the magnetized plasma. Moreover, when the ISMF strength is decreased to values actually observed by *V1* beyond the HP (4–6 μG) (Burlaga et al. 2013), or, since the draped field near the HP can be stronger than the undisturbed ISMF (by ∼40% if the field is as weak as ∼3 μG), to even lower values (3 μG or 2.7 μG, Grygorczuk et al. 2011; Heerikhuisen et al. 2014; BenJaffel et al. 2013), the draped field near the *V1* direction in our heliographic projection remains similar enough in structure to the idealized model (Figure 3) to agree approximately with *V1* observations. The red line in Figure 1 shows the draped field line obtained for the ISMF of 4 μG. The angle between the red line and the heliographic parallel passing through the *V1* direction is larger than for the idealized draping model (the blue line). However, this is consistent with *V1* observations which correspond to the small but nonzero angle between the field outside and inside HP.

To agree with the *V1* measurements, the red line at the *V1* position should be strictly tangent, not to the heliographic parallel, but to the ($V1$, B_{OUT}) plane (defined by the *V1* direction and the direction of the magnetic field measured by *V1* outside the HP). In our projection, this plane is represented by the great circle passing through the points *V1* and B_{OUT}. Figure 1 shows that the draped field line corresponding to our draping model for an ISMF strength of 4 μG is indeed close to being tangent to this great circle. Moreover, the draped field direction in space derived from the model B^{V1}_{mhd} (the red square) is close (∼10°) to the measured field direction B_{OUT} (the black square).

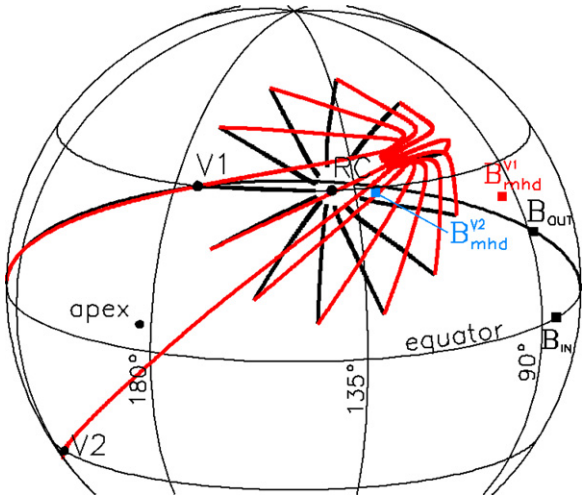

Figure 3. Comparison of draped interstellar magnetic field lines from our simulations for field strengths of 20 and 3 μG (black and red, respectively). The lines originate from selected points just outside the heliopause, distributed over a circle of radius 27° with the same center as the *IBEX* ribbon.

Figure 1 also shows the heliographic parallel and the magnetic field line for the idealized draping model passing through the *V2* position. The angle between the field line and the parallel is clearly large (30°), implying that the solar magnetic field and the draped ISMF will not be close in direction along the *V2* trajectory. Similar values (∼32° and 31°) are obtained in our 3D MHD simulations for ISMF strengths of 4 and 3 μG, respectively. The angular distance between the *V2* position and the RC is also much larger (∼97°) than for *V1*.

The vicinity of the *V1* direction is not the only region where the magnetic fields outside and inside the HP can be parallel (or antiparallel) to each other. In the idealized draping model, each of the ISMF lines becomes tangent to a heliographic parallel at two points. The dashed blue line in Figure 1 shows a locus of such points situated between the north pole and the ISMF directions (a similar line appears in the southern hemisphere). The draped field line that crosses this oval becomes tangent to the heliographic parallel at the crossing point (as illustrated by the elongated blue line in the north). If a spacecraft trajectory direction were close to this line, then, assuming the idealized draping model, the solar and interstellar fields observed at the HP would be approximately parallel (or antiparallel, for opposite polarity of the solar field). The actual direction of the *V1* trajectory (at the same solar latitude and close in longitude to the RC) satisfies this condition.

3. MHD MODELS

3D MHD simulations for the case of a star moving through a strongly magnetized (up to 20 μG) interstellar medium also including the plasma and neutral gas components (Czechowski et al. 2014) led to a two-stream structure of the stellar plasma flow. In this case, the streams (containing most of the plasma flow) are slightly deflected from the interstellar field direction. The rest of the outflowing stellar plasma forms a tail opposite to the stellar motion. The two stream structure becomes less pronounced for larger values of the neutral interstellar hydrogen density. Nevertheless, the draping structure for the strong interstellar field case (Figure 3, black arcs) remains similar to our simple draping model (Figure 1, blue lines).

After crossing the HP, *V1* is observing an interstellar field strength between 4 and 6 μG. To check the draping structure for the ISMF in this range, we performed a 3D MHD simulation for the local field strengths of 6, 5, 4, 3, and 2.7 μG, with the asymptotic field directed toward the *IBEX* RC. We found that the weaker the field, the more its draping structure differs from that of the strong (20 μG) field case. Figure 3 illustrates this difference for an ISMF strength of 3 μG. Although the draped field is not as simple as for the 20 μG case, in our region of interest (between the undisturbed field (RC) and *V1* direction) its structure simplifies and takes the form consistent with *V1* magnetic field measurements. As explained above, the draped magnetic field line passing through the *V1* trajectory is close to tangent to the plane defined by the *V1* and B_{OUT} directions, and close in direction to the solar magnetic field on the inner side of the HP.

Table 2
Boundary Conditions for MHD Calculations[a]

LISM Parameters					Solar Wind Parameters[b]	
B_{IS} (μG)	T_{IS} (K)	n_{IS} (cm^{-3})	n_H (cm^{-3})	V_{IS} (km s^{-1}) Slow/Fast	$V_{SW,1\ AU}$ (km s^{-1}) Slow/Fast	$n_{SW,1\ AU}$ (cm^{-3})
20	6300	0.04	0.1	23.2	750	4.2
4, 5, 6	6300	0.06	0.1	23.2	400	5.55
2.7, 3, 4, 5	6300	0.06	0.1	23.2	400/750	5.55/1.58
3, 4	6300	0.06	0.1	23.2	500/750	5.55/2.46

Notes.
[a] The inner boundary of the calculation region is at 15 AU, the outer at 5849 AU from the Sun.
[b] In the slow/fast solar wind cases, the slow wind flows within 36° of the solar equator.

The direction of the draped magnetic field in space at the *V1* position following from our models depends on the assumed ISMF strength. For a very strong field (20 μG) it is different from the *V1* result B_{OUT}, but for the weaker and more realistic ISMF strength values it becomes close to B_{OUT} (within about 10°). At the same time, the angle between the draped magnetic field at *V1* and the heliographic parallel increases from a low value (less than 10°) obtained for the idealized draping model and for a strong ISMF (20 μG) to a somewhat higher value (15°, close to *V1* observations) for the realistic ISMF.

In our calculations, we use a 3D MHD time-stationary numerical code describing the interaction of the solar wind with the LISM (boundary conditions for our models are shown in Table 2). The parameters of the solar wind are based on Ulysses data (Ebert et al. 2009). The interstellar medium parameters were chosen to agree with observations from the *IBEX* and *Voyager 1* spacecraft (Gurnett et al. 2013), and model estimations. The code employs a fixed grid. A uniform flux of neutral hydrogen is assumed (Bzowski et al. 2009; Ratkiewicz & Grygorczuk 2008). The solar magnetic field is disregarded to limit undesired numerical effects (like artificial diffusion of the magnetic field at the HP) that could affect the HP region. In effect, as in ideal MHD case, we assume that there is no coupling between the magnetic fields across the HP.

We use the models to obtain the shape of the HP and the structure of the draped magnetic field. Since the HP in our models is not a discontinuity but a transition of finite width, we cannot reliably calculate the behavior of quantities like the magnetic field strength or plasma density with distance in vicinity of the HP. For the magnetic field direction, we find that the agreement of the 4 μG and 3 μG cases with *V1* observations is satisfactory. The calculated ISMF direction at *V1* just outside

the HP (the red squares marked $B_{\rm mhd}^{V1}$ in Figures 1 and 3) is deflected by $\sim 11^\circ$ from the observed direction. While the distance to the HP is overestimated, the obtained termination shock distances at *V1* and *V2* are within a few percent of the measured ones (Stone et al. 2005, 2008) when the slow wind speed is taken to be 500 km s^{-1}, but smaller (by less than 20 %) for a slow wind speed of 400 km s^{-1}.

4. DISCUSSION AND CONCLUSIONS

Throughout this paper, we use the heliographic projection. We are interested in the magnetic field lines near the HP. The inner and outer magnetic fields are then draped over the same surface. Since the HP is not strictly perpendicular to the radial direction, the angles between the projected field lines are not the same as the angles between the field lines in space. However, as long as we exclude the case of a HP tangent to the radial direction, the lines draped over the same element of the HP and strictly parallel (antiparallel) in projection also have the same property in space. We can therefore restrict attention to the heliographic projection and do not have to specify the shape of the actual HP. If the considered part of the HP is not very far from being perpendicular to the radial direction, then the field lines forming a small angle in projection will also form a small angle in space.

Our results clarify the cause of similar magnetic field directions on both sides of the HP, as observed by *V1*: the heliographic latitude of *V1* happens to be the same as that of the undisturbed ISMF (to be given by the *IBEX* RC). We have shown that for the wide range of ISMF strength values, including those actually observed by *V1* beyond the HP, the draped interstellar field near the *V1* trajectory (calculated with zero heliospheric magnetic field to avoid artificial field diffusion across the boundary) must then be close in direction to the solar inner heliosheath magnetic field. For realistic ISMF strength values, our model results obtained for the draped field direction in space are within 10° of *V1* observations beyond the HP. For *Voyager 2*, we predict that the difference between the inner and the outer magnetic field directions at the HP will be significantly larger than that observed by *Voyager 1* ($\sim 30^\circ$ instead of $\sim 20^\circ$) and that the outer field direction will be close (7°–9° off) to the RC.

This explanation is natural and simple, and removes the only objection against the claim that *V1* reached the interstellar medium. It supports the interpretation of the RC as the direction of the undisturbed ISMF, with the ISMF oriented toward the northern hemisphere. It is consistent with the classical picture of the HP not being dominated by turbulence or reconnection effects. The reasonable agreement between *V1* and our results for the magnetic field direction gives us confidence that the results are not affected by the approximations inherent to our models.

Approximate agreement with *V1* magnetic field measurements was also achieved in numerical models that differ significantly from our approach. Borovikov & Pogorelov (2014; see also Pogorelov et al. 2009), who take HP instability into account, obtain a solution in which *V1* is moving through a local interstellar plasma intrusion, partly surrounded by the heliosheath plasma. They predict that *V1* may re-enter the heliosheath in the near future. Opher & Drake (2013), from numerical calculations that include both solar and interstellar magnetic fields, conclude that the presence of the solar magnetic field strongly affects the draping of the ISMF over the HP. In their solution, for different assumptions concerning the undisturbed ISMF, the draped ISMF is close in direction to the heliospheric magnetic field in a large area of the HP also including the *V1* and *V2* trajectory directions. Calculations of Borovikov & Pogorelov (2014) do not confirm this result. The solar field assumed by Opher & Drake (2013) is very simplified. In particular, the sector polarity structure is ignored. Contrary to Opher & Drake (2013), we assume that the solar magnetic field does not strongly affect the shape of the HP and the draping pattern. The similarity of the field directions on both sides of the HP follows from the relative directions of *V1* and the undisturbed ISMF.

This work was supported by the Polish National Science Center grant 2012-06-M-ST9-00455. A.C. acknowledges participation in ISSI International Team 291.

REFERENCES

BenJaffel, L., Strumik, M., Ratkiewicz, R., & Grygorczuk, J. 2013, ApJ, 779, 130
Borovikov, S. N., & Pogorelov, N. V. 2014, ApJL, 783, L16
Burlaga, L. F., Ness, N. F., Gurnett, D. A., & Kurth, W. S. 2013, ApJL, 778, L13
Burlaga, L. F., Ness, N. F., & Stone, E. C. 2013, Sci, 341, 147
Bzowski, M., Moebius, E., Tarnopolski, S., Izmodenov, V., & Gloeckler, G. 2009, SSRv, 143, 177
Czechowski, A., Grygorczuk, J., McComas, D., & Ratkiewicz, R. 2014, A&A, submitted
Ebert, R. W., McComas, D. J., Elliott, H. A., Forsyth, R. J., & Gosling, J. T. 2009, JGR, 114, 1109
Fisk, L. A., & Gloeckler, G. 2013, ApJ, 776, 79
Florinski, V. 2013, arXiv:1302.2179v1
Fränz, M., & Harper, D. 2002, P&SS, 50, 217
Funsten, H. O., Allegrini, F., Crew, G. B., et al. 2009, Sci, 326, 964
Funsten, H. O., De Majistre, R., Frisch, P. C., et al. 2013, ApJ, 776, 30
Grygorczuk, J., Ratkiewicz, R., Strumik, M., & Grzedzielski, S. 2011, ApJL, 727, L48
Gurnett, D. A., Kurth, W. S., Burlaga, L. F., & Ness, N. F. 2013, Sci, 341, 1489
Heerikhuisen, J., Zirnstein, E. J., Funsten, H. O., Pogorelov, N. V., & Zank, G. P. 2014, ApJ, 784, 73
McComas, D. J., Allegrini, F., Bochsler, P., et al. 2009, Sci, 326, 13
McComas, D. J., Dayeh, M. A., Funsten, H. O., Livadiotis, G., & Schwadron, N. A. 2013, ApJ, 771, 77
McComas, D. J., & Schwadron, N. A. 2012, ApJ, 758, 19
Opher, M., & Drake, J. F. 2013, ApJL, 778, L26
Parker, E. N. 1961, ApJ, 134, 20
Pogorelov, N. V., Borovikov, S. N., Zank, G. P., & Ogino, T. 2009, ApJ, 696, 1478
Ratkiewicz, R., & Grygorczuk, J. 2008, GeoRL, 35, L23105
Schwadron, N. A., & McComas, D. J. 2013, ApJL, 778, L33 9
Stone, E. C., Clummings, A. C., McDonald, F. B., et al. 2005, Sci, 309, 2017
Stone, E. C., Clummings, A. C., McDonald, F. B., et al. 2008, Natur, 454, 71
Stone, E. C., Cummings, A. C., McDonal, F. B., et al. 2013, Sci, 341, 150